JUNE 1978 LRP 141/78

# A 40 JOULE $CO_2$ TEA LASER MODULE WITH A UNIFORM-FIELD ELECTRODE PROFILE AND SIDE-ARC PREIONIZATION

M.R. Green, P.D. Morgan, M.R. Siegrist

# A 40 Joule $CO_2$ TEA Laser Module with a Uniform-Field Electrode Profile and Side-Arc Preionization

M.R. Green, P. D. Morgan, M.R. Siegrist

Centre de Recherches en Physique des Plasmas
Ecole Polytechnique Fédérale
CH-1007 Lausanne / Switzerland

## Abstract

The design of a TEA $CO_2$ laser is described. This compact device (discharge volume 100 x 5 x 5 cm) produces up to 40 Joules in a pulse of duration 30 nsec. The gas is preionised by u.v. irradiation from a self-synchronising system of capacitively-coupled arc discharges along the sides of the uniform field-electrodes. Beam homogeneity and pulse reproducibility are both excellent.

TABLE OF CONTENTS

List of Tables and Figures



Figures

## Introduction

Since the first demonstration in 1969[1] of a transversely-excited $CO_2$ laser operating at atmospheric pressure, steady progress in the performance of such lasers has been achieved[2].

Two significant advances have been reported recently in the design of these lasers, making it relatively simple to achieve uniform discharges in large-volume TEA lasers. The first is the achievement of good preionization of the gas by intense u.v. irradiation from capacitively-coupled arcs initiated along the sides of the main discharge[3]. The benefits arising from the use of this self-synchronising system are:

i high-energy-density pumping is achieved in the main discharge with reliable arc-free performance and uniform excitation,

ii high gain is achieved, with the capabilities of large outputs of energy and power,

iii reliable performance is achieved over a wide range of gas mixtures.

Secondly, a uniform-field electrode profile has been derived by Chang[4] in terms of simple analytic formulae, permitting ease of manufacture of the electrodes using cutting tools fabricated on a computer-controlled machine. The use of Chang profile electrodes of suitable aspect ratio results in output beams with a high degree of homogeneity over a large fraction of the discharge cross-section.

We describe the design and performance of a laser which incorporates both of the features described above.

## Laser Module Design

### a. Preionization

The gas is preionized prior to the main discharge by intense ultraviolet irradiation produced by an array of hot arcs along each side of the electrodes. The arcs are formed between opposing steel pins, capacitively coupled to the electrodes by 570 pF capacitors, arranged at 4 cm intervals along the full length of the Chang-profiled electrodes (Figs. 1,2,3). Using this arrangement, the appropriate delay between the generation of the u.v. light and the occurrence of the main electrical discharge is automatically achieved, without recourse to auxiliary circuitry, when the discharge circuit is switched[3,5]. P.V.C. shields are located between the arrays of preionization capacitors and the electrodes to prevent electrical tracking across the capacitors to the electrodes and consequent degradation of the laser performance.

### b. Electrode Design

The successful operation of a large-volume TEA $CO_2$ laser depends on attaining a uniform glow discharge over the entire active volume. Currently, an optimal way of achieving this is to employ a combination of intense u.v. irradiation to preionize the active medium, as already described, and of specially-shaped large-area electrodes where the electric field between them is kept as uniform as possible to inhibit arcing.

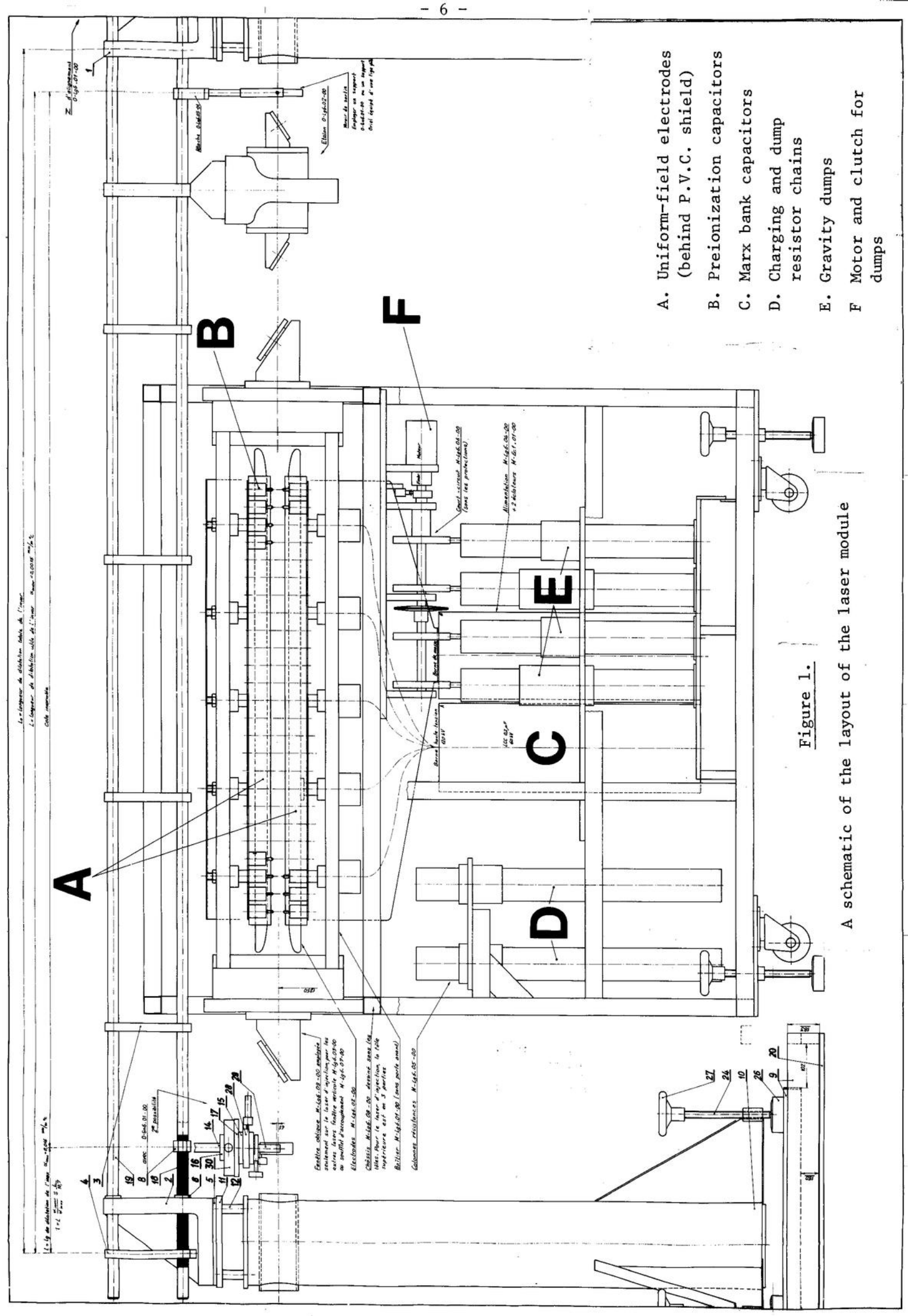


A. Uniform-field electrodes (behind P.V.C. shield)

B. Preionization capacitors

C. Marx bank capacitors

D. Charging and dump resistor chains

E. Gravity dumps

F Motor and clutch for dumps

Figure 1.

A schematic of the layout of the laser module

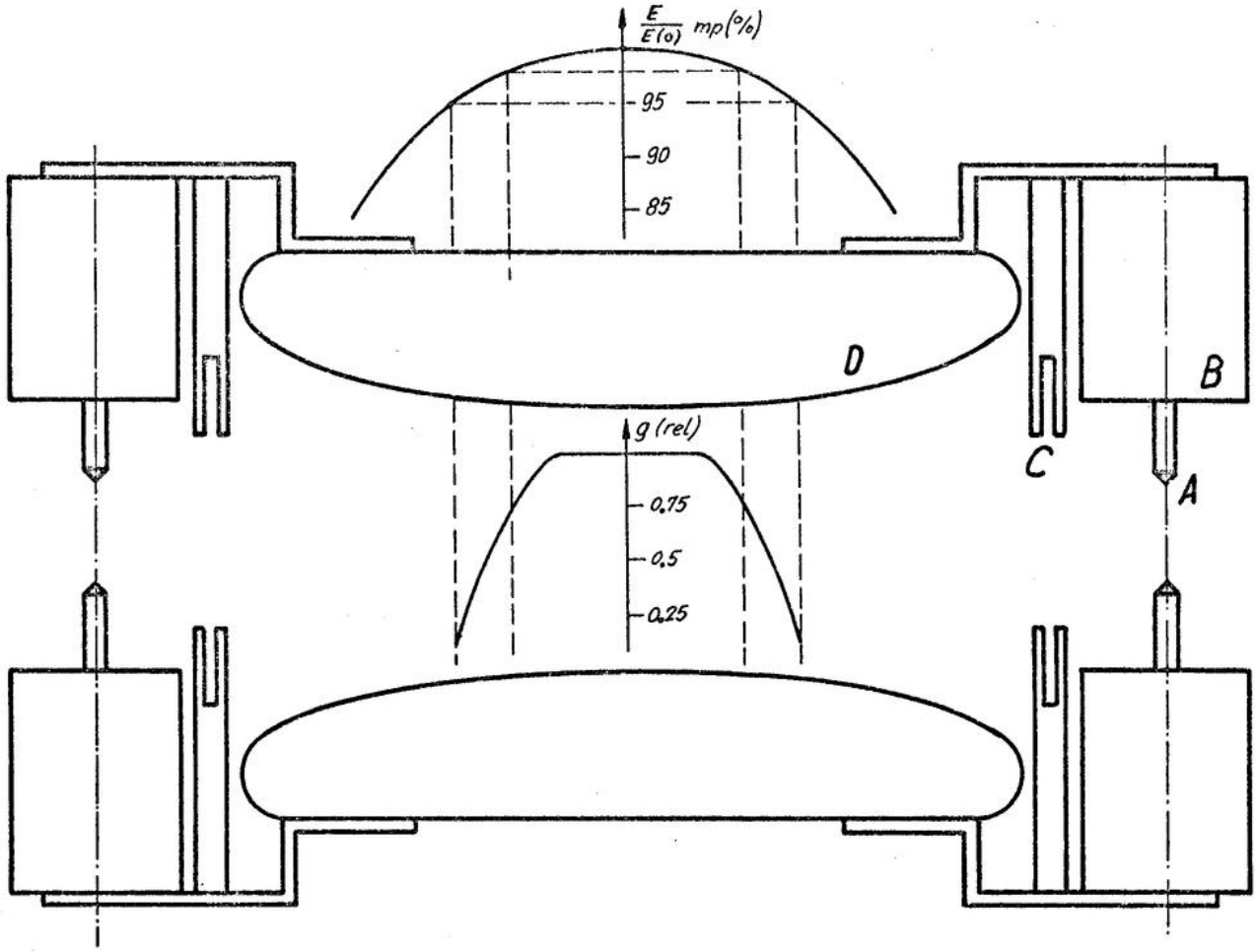


Figure 2.

A schematic drawing of the Chang electrodes showing preionization arrangement and calculated values of relative gain and $E/E_o$.

A. Electrodes for preionization discharge

B. Preionization capacitors

C. P.V.C. shield

D. Uniform-field electrodes

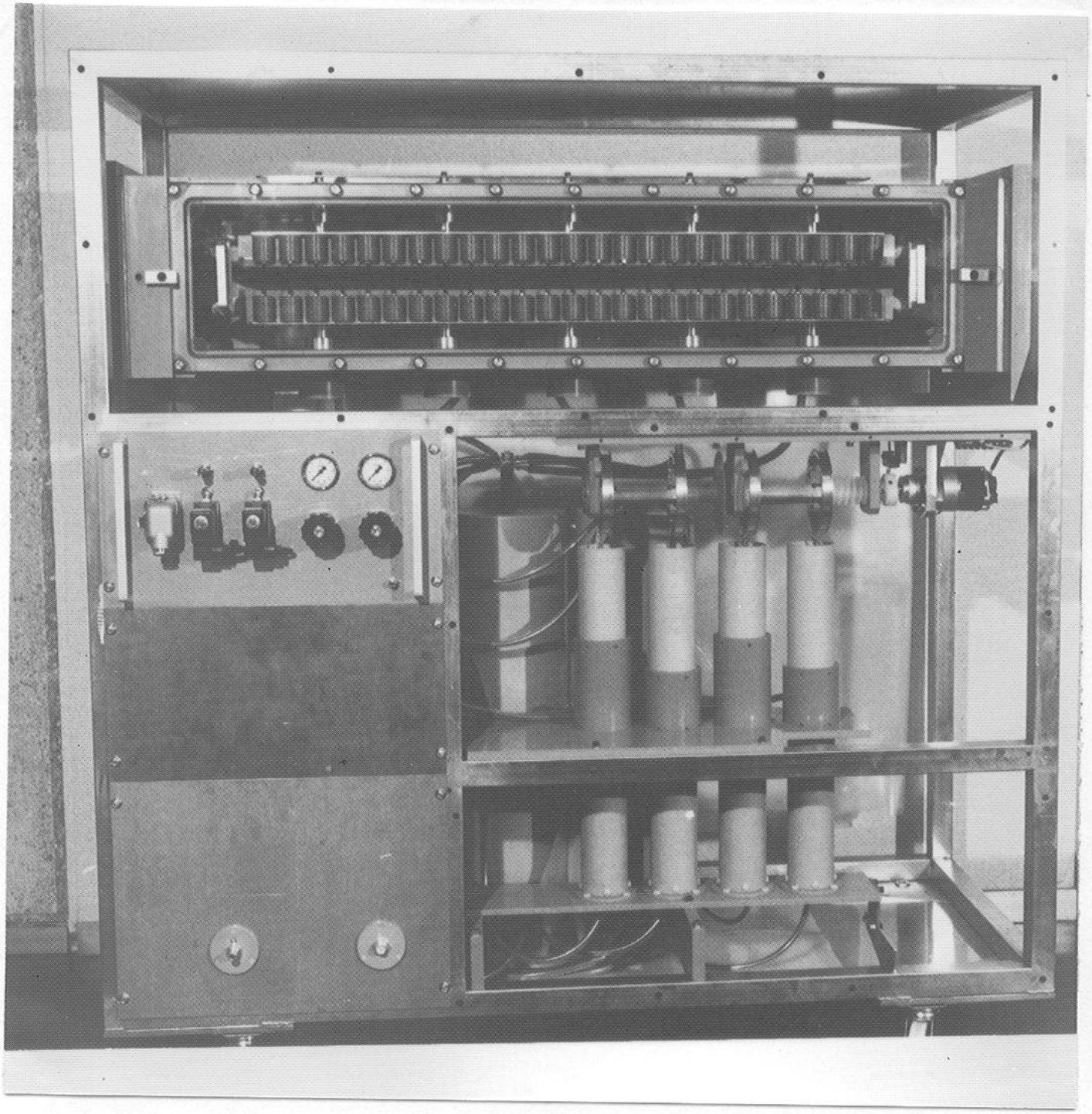

Figure 3.

A photograph of the laser module with the side panels removed.

The uniform-field electrodes most commonly used have a Rogowski profile. In cross section the profile is made up of three individual segments taken from an infinitely-wide analytic profile - a flat centre section joined abruptly to curved edges. Less common are the Bruce profile, which is purely an empirical approximation, and the Harrison profile, which is a numerical compromise between the previous two. All three profiles are rather arbitrary approximations of a true uniform-field electrode. It is difficult to improve any of these profiles from its present state because the electric field distribution cannot be described analytically.

Recently a new type of uniform-field electrode has been described by Chang, which employs simple analytic formulae to define the profile for any desired field uniformity. For a given electrode width and thickness, only the curvature at the extreme edges of the profile need be non-analytically described; a consequence of the finite electrode dimenstions. The Chang profile, in fact, simultaneously achieves a compactness, a smoothness and a uniformity of electric field that are not approached by any of the other three profiles.

For Chang's uniform-field electrode of finite width, the profile of any equipotential surface corresponding to a certain value v of the potential function and a value u of the flux function, which is a variable, is given by

$$a = u + k \cos v \sinh u \qquad (1)$$

$$y = v + k \sin v \cosh u \qquad (2)$$

At the point (0,0), which corresponds to the exact centre of the discharge cross section between the two electrodes, the x direction is parallel to the surfaces of the electrodes and the y direction is perpendicular. k is a parameter describing the physical curvature of the electrode surface - in general, the larger the value of k the more curved is the electrode profile. We choose the largest value of k consistent with obtaining the required electric field uniformity, i.e. we compromise between compactness and perfect uniformity.

The electric field, in dimensionless units, is given by

$$E^{-2} = (1 + k \cos v \cosh u)^2 + (k \sin v \sinh u)^2 \quad . \qquad (3)$$

We obtain the potential function $v_o$ at the electrode surface from the condition $\partial^2 E^{-2}/\partial u^2 = 0$ at $u = 0$. Using this and equation (3), we obtain

$$v_o = \pi/2 + \sin^{-1} k \quad . \qquad (4)$$

Putting the above value of $v_o$ in equation (2), with $u = 0$, we obtain the separation $y_o$ of each electrode surface from the point (0,0)

$$y_o = v_o + k \sin v_o \quad . \qquad (5)$$

The electrode profile is calculated from equations (1) and (2), i.e. for different values of x we compute the corresponding values of y. With $v = v_o$, equation (1) is solved iteratively to yield the value of u corresponding to a certain value of x. This value of u is then used in equation (2), with $v = v_o$, to obtain the value of y. Finally the x and y values are normalized to the actual required separation of the electrodes $2y_o'$ by multiplying each value by $y_o'/y_o$.

In Figure 2 we plot the profile chosen for the electrodes of the TEA $CO_2$ laser. The edges of the electrode profile are circular in cross section with radius 8 mm, smoothly joined to the Chang profile on one side and a flat surface on the other. Also shown is a plot of the variation of the electric field strength along the midplane, normalized to the field strength at the centre of the cross section, i.e. $E(x,0)/E(0,0)$. The latter plot was derived using equation (3), with a value of u corresponding to $y = 0$ and $v = 0$. We see that over a width of 4 cm, centred on $x = 0$, the field strength does not vary by more then 2%. This was achieved for the electrode separation of 5 cm by

employing a value of k of 0.02. Such uniformity is necessary since it was demonstrated by Robinson[5] that the gain of such a laser operating at 120 kV varies along the midplane according to the electric field strength, and that the gain has decreased to 50% of maximum at the point where the electric field has decreased by 4%.

The electrodes are made from "anticorrodal" aluminium (Al-Mg with 1% Si) on a milling machine, using a cutting tool fabricated to have the appropriate profile on a numerically-controlled machine. An electrode consists of a one meter long section of constant width terminating in two semicircular ends, each of radius equal to half the width, profiled by the cutting tool.

It was observed that in the case of the prototype laser module, in addition to the main laser beam, two parasitic beams were produced due to reflections off the polished electrode surfaces. Consequently, the finished electrodes are sand blasted with fine-grain sand until the surfaces have a matt finish. This treatment reduces the parasitic modes considerably. It was found that the parasitics could be eliminated, without degrading the laser performance, by covering each electrode surface with a single layer of glass fibre cloth woven from 0,5 mm diameter strands.

c. Discharge Circuit

A schematic of the discharge circuit, which consists of a two-stage Marx bank, is shown in Figure 4. Each stage comprises a 0.22μF capacitor, a switch, a 400 kΩ ballast resistor and a gravity-acting resistive dump and short circuit. Essentially, the capacitors are charged in parallel, to a maximum of 60 kV, then discharged in series to produce a pulse of double the charging voltage across the electrodes. Switching is achieved with two low-inductance three-electrode spark gaps[6].

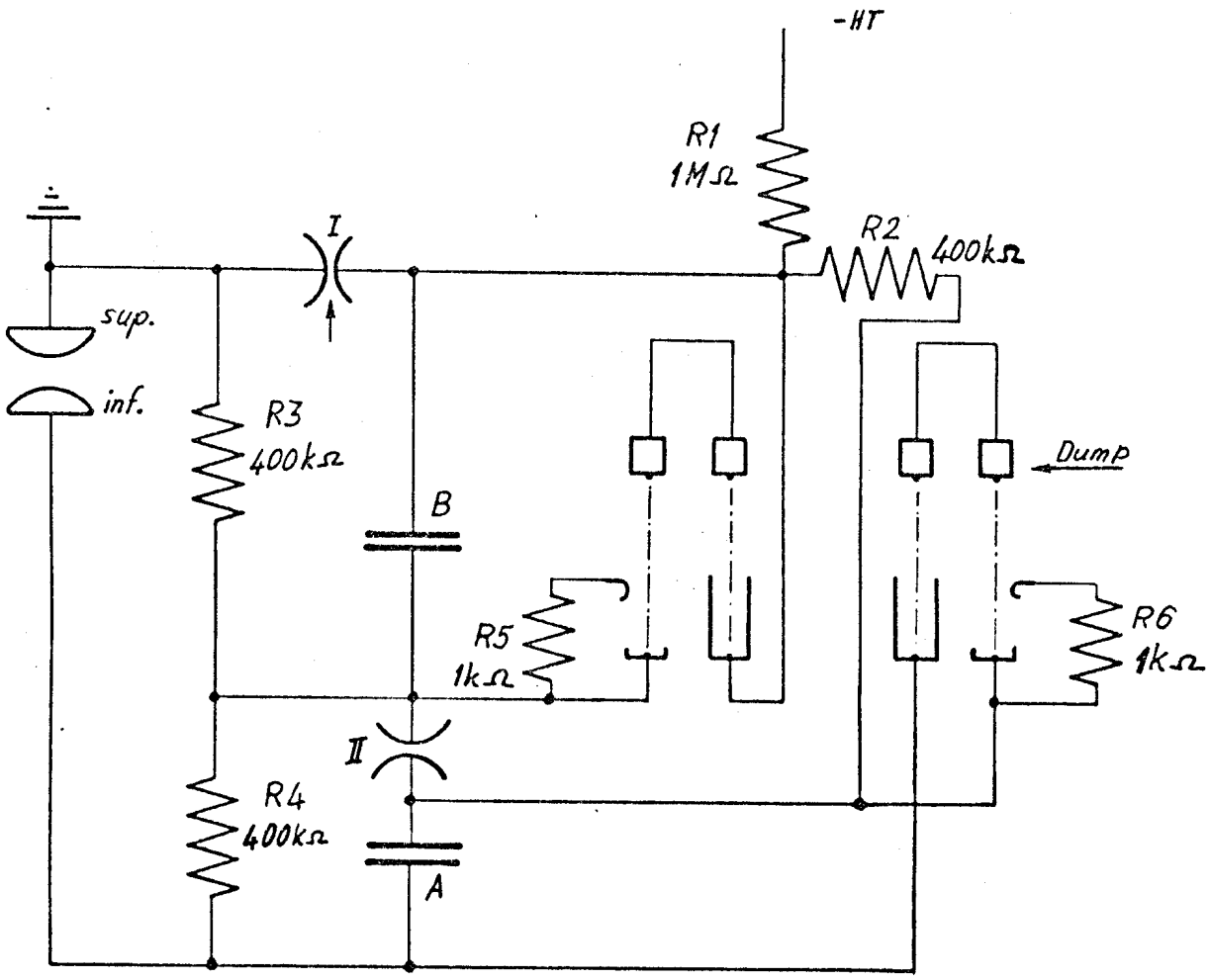


Figure 4. A schematic of the laser discharge circuit

Spark gap I is triggered by applying a 80 kV pulse to its centre electrode, resulting in the potential across spark gap II being doubled and, consequently, prompt breakdown.

The cylindrical capacitors are mounted side by side, in an upright position, with spark gap II connecting their lower terminals. The upper terminal of capacitor A is connected to the lower electrode (the anode) of the laser via five thick cables of equal length. A metal sheet, the current return, connects the upper electrode to the upper terminal of capacitor B, via spark gap I.

The resistors are so arranged that the voltage across any one of them never exceeds the charging voltage on the capacitors. An appropriate number of low voltage resistors in series, enclosed in insulating tubes constitute the ballast and charging resistors. The dump resistors are made up of heavy duty ceramic resistors and are designed to withstand the repeated dissipation of the charge on the capacitors without damage.

Each of the two gravity dumps consists of a pair of pistons, enclosed in insulating tubes, which are lifted by a common shaft driven by an electric motor. Interruption of the electric power to the motor, due to power failure, interruption of the safety interlock system or operation of the emergency dump switch, decouples the shaft from the motor. The free-falling weights first encounter a contact which discharges the capacitors through the dump resistors, finally coming to rest on a contact which forms a short circuit.

The electrical characteristics of the module are summarized in Appendix B.

d. Power Supply

The D.C. power supply is essentially a 220 to 23000 volt step-up transformer together with a rectifier consisting of a cascade voltage doubler. Output voltages from 100 to 60,000 volts can be selected in steps of 100 volts, at a maximum current of 30 mA. The voltage is stabilized to within ± 30 volts of the selected value.

A schematic diagram of the supply is shown in Fig. 5. Coarse voltage control is achieved by varying the volts applied to the primary of the H.T. transformer, using a motor-driven variable-turn transformer of the variac type. Fine voltage control is achieved by varying the portion of the mains voltage cycle over which volts are applied to the primary of the H.T. transformer, using a triac as a switching device. The output voltage, suitably attenuated, is compared with the value selected using a comparator, and the switching of the triac and the setting of the variac are adjusted until the correct voltage is achieved.

Performance : Experimental Results

The main feature of the laser is its extremely reliable operation over a wide range of gas mixtures. Over the 5 x 5 cm discharge cross-section the homogeneity of the output beam is excellent, as can be seen from a burn mark recorded on a piece of developed, unexposed Polaroid film, Figure 6.

The performance of the laser at various voltages and for a variety of gas mixtures is summarized in Table 1. Premixed gases* were used, and flow rates of 1 - 2 litres per minute through the airtight gas chamber were adequate for repetition rates of up to 2 shots per minute. If the chamber had been exposed to air it was found necessary to flush it out for several hours, as even small amounts of oxygen in the chamber resulted in arcing. When using mixtures that were rich in $CO_2$, it was necessary to

*see Appendix D

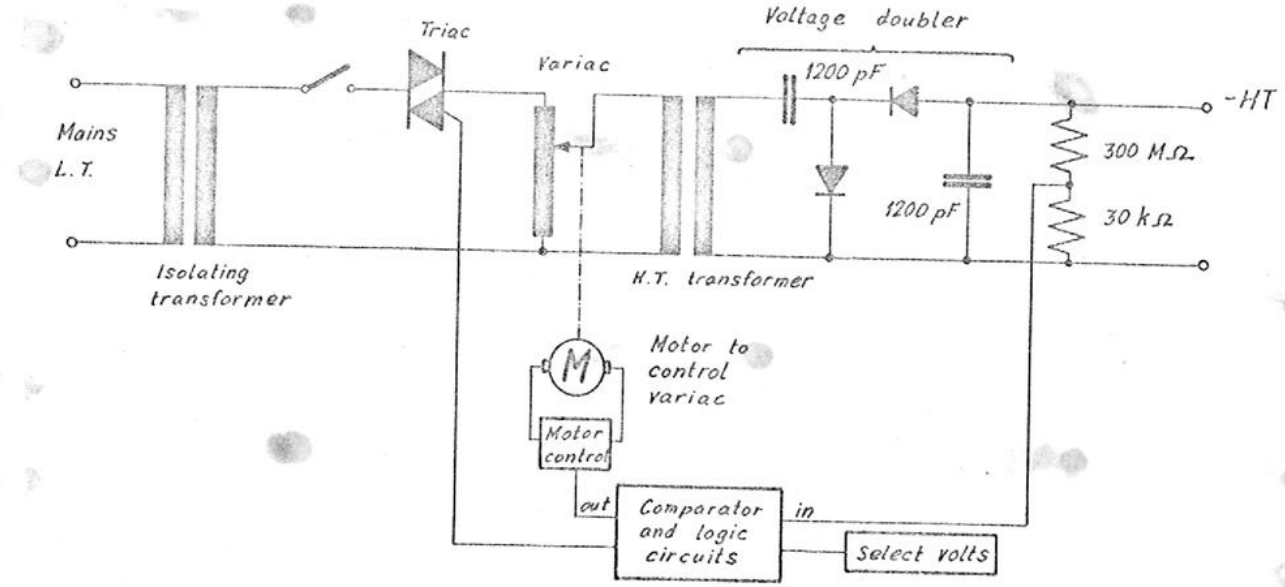


Fig. 5. Schematic diagram of laser power supply

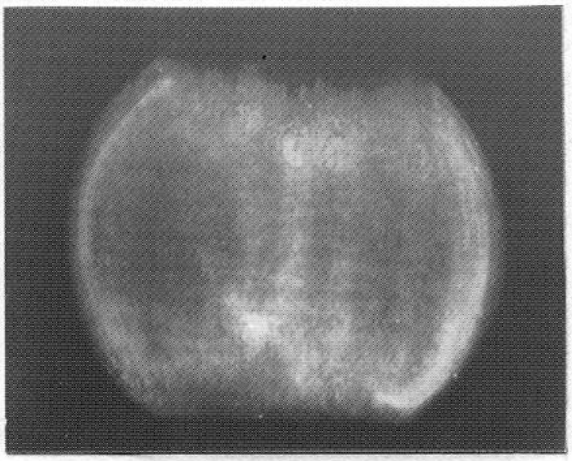

Fig. 6. A burn mark on an unexposed, developed Polaroid film

| Gas Mixture $CO_2$:$N_2$:He | Additive | Charging Volts (kV) | Spike Energy (J) | Tail Energy (J) | Total Energy (J) | Ratio: Spike/Total | Spike FWHM (ns) | Tail Length(ns) | Spike Power (MW) |
|---|---|---|---|---|---|---|---|---|---|
| 25:25:50 | no | 45 | 26 | 17 | 43 | 0.6 | 29 | 910 | 896 |
| 25:25:50 | no | 50 | 21 | 32 | 53 | 0.4 | 35 | 1000 | 600 |
| 25:25:50 | no | 55 | 18 | 38 | 56 | 0.3 | 30 | 990 | 600 |
| 30:15:55 | no | 50 | 17 | 25 | 42 | 0.4 | 30 | 840 | 510 |
| 30:30:40 | yes | 50 | 37 | 16 | 53 | 0.7 | 31 | 670 | 1200 |
| 35:15:50 | no | 50 | 24 | 15 | 39 | 0.6 | 34 | 500 | 710 |
| 35:40:25 | yes | 50 | 39 | 22 | 61 | 0.6 | 30 | 880 | 1300 |
| 40: 0 :60 | no | 50 | 18 | 5 | 23 | 0.8 | 30 | 440 | 600 |
| 45: 0 :55 | yes | 50 | 7 | 0 | 7 | 1.0 | 50 | 0 | 130 |

Table I Various laser pulse parameters as a function of gas mix and charging voltage.

All energy measurements were made using a Gen Tec Pyro-electric Joulemeter type ED 500.

All temporal measurements were taken using a Photon Drag (Rofin. Type 7400) and a Tektronix 7400 oscilloscope (7A19 Plug-in).

add tri-n-propylamine vapour to the gas mixture to suppress arcing[7]. Gas saturated with vapour was obtained by diverting one tenth of the gas flow and bubbling it through a bath of the liquid. The container walls were opaque to prevent photochemical processes occurring as these eventually degrade the performance of the additive.

In the first three rows of Table I the characteristics of the output are compared for three different charging voltages with a gas mixture of $CO_2$:$N_2$:He in the ratio 25:25:50. The total energy increases with increasing voltage V, but the energy in the spike actually decreases as V increases. The effect of varying the gas mixture at constant voltage is contained in rows 4 to 7 of the table. It can be seen that the spike energy increases with increasing $CO_2$ content; also for fixed $CO_2$ content the spike energy increases with increasing $N_2$ content. The final two rows illustrate that the tail can be eliminated, or reduced to low levels, by using a nitrogen-free mixture. However, the power is much reduced.

It can be seen from Table I that the duration of the output spike is largely the same for all the gas mixtures, averaging 31 nsec FWHM, except for the final nitrogen-free mixture. Typical traces of the $CO_2$ laser output are shown in Figure 7, recorded with a photon-drag detector. The cavity used, in all cases, comprised a gold-coated concave mirror of focal length 250 cm and an uncoated NaCl flat.

A trace of the current and voltage waveforms is shown in Figure 8, with a time scale of 200 nsec/cm. The initial voltage spike indicates the formation of the side-arcs. For $\sim$160 ns the preionization capacitors charge up through the resistance of the arcs as indicated by a simultaneous rise of current and voltage. During this time the main discharge volume is irradiated by intense UV light emitted from the arcs. When the voltage reaches breakdown threshold ($\sim$80 kV) in the preionized gas, the

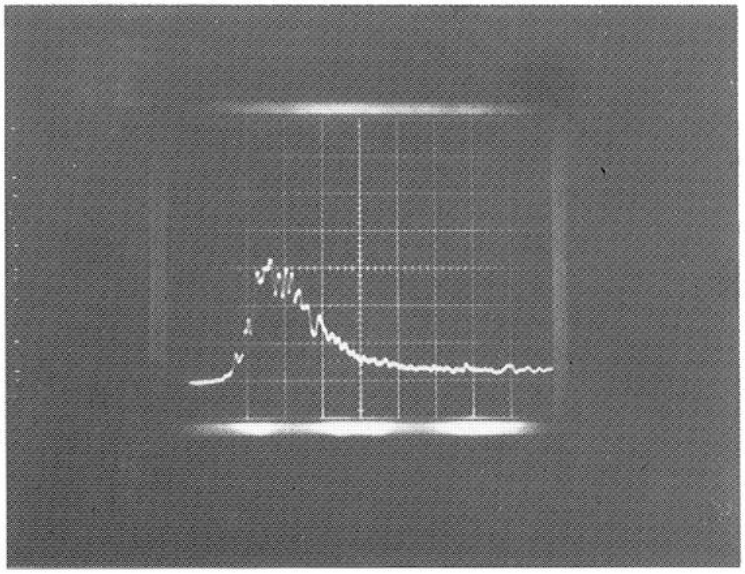

Fig. 7.a) Typical oscilloscope traces of the laser output

100 mV/div; 20 nsec/div.

time →

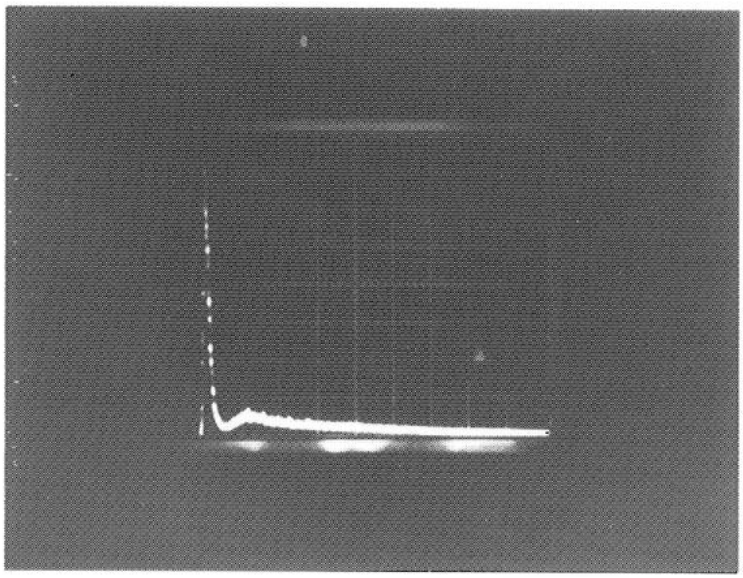

Fig. 7.b) Typical oscilloscope traces of the laser output

50 mV/div; 200 nsec/div.

time →

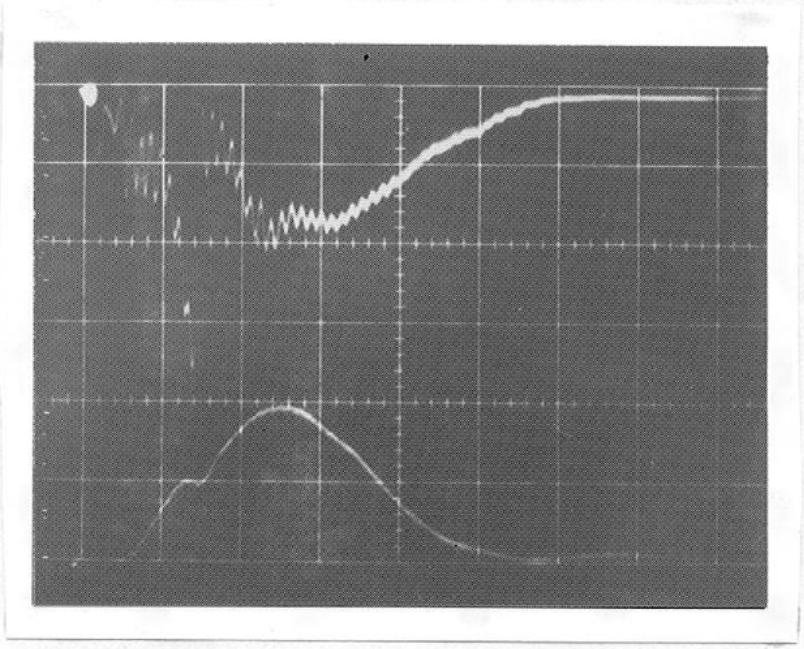

Fig. 8. An oscilloscope trace of the voltage (upper) and current (lower) during a discharge. Vertical scale 30.5 kV and 7.8 kA/major division, respectively. Horizontal scale 200 nsec/cm.

main discharge commences. This results in a rapid voltage drop across the electrodes. Current and voltage traces now display the characteristics of an overdamped RLC circuit. The voltage builds up to a secondary maximum at the current maximum of ∿18 kA and then decays on the same time scale as the current. If the side-arcs are not extinguished at the onset of the main discharge or if they strike again part of the energy stored in the preionization capacitors is fed into the main discharge.

## Summary

A description has been given of the design, construction and performance of a compact TEA $CO_2$ laser module. Uniform-field electrodes with a Chang profile are employed to excite the 2.5 litre active volume, which is preionized by means of a row of capacitively-coupled arc discharges along each side of the electrodes. Energies of up to 40 Joules in a pulse of duration ∿30nsec have been achieved, with excellent beam homogeneity and pulse reproducibility.

Acknowledgements

The authors wish to acknowledge the excellent assistance rendered in the course of this project by the technical services of the C.R.P.P. In particular, they wish to thank J.-M. Mayor of the drawing office, R. Dussault and the staff of the mechanical workshop, S. Bersier and G. Bochy of the electrical workshop and R. Gribi and C. Rizzo of the electronics laboratory.

The continual support and encouragement of this project by A. Heym is much appreciated.

Finally, the authors wish to thank A.A. Offenberger of the Electrical Engineering Department, University of Alberta, Canada for providing much useful information pertaining to the construction of the laser.

This work was supported by the Swiss National Science Foundation.

References

1 Dumanchin, R., and Rocca-Serra, J.,
C.R. Acad. Sci. 269, 916 (1969)

2 Wood, O.R., Proc. IEEE 62 (3), 355 (1974)

3 Burnett, N.H., and Offenberger, A.A.,
J. Appl. Phys. 44 (8), 3617 (1973)

4 Chang, T.Y., Rev.Sci.Instr. 44 (4), 405 (1973)

5 Robinson, A.M., J.Appl.Phys., 47 (2), 608 (1976)

6 Barnes, P.M., Gruber, U.W., and James, T.E.,
Culham Laboratory Report CLM-R71 (1967)

7 Lietti, A., CRPP Lausanne, LRP 135/78
"The Influence of Additives and Contaminants in TEA $CO_2$ Laser Discharges Evaluated by Electrical Measurements"

Appendix A

## Laser Head Characteristics

| | |
|---|---|
| Electrode type | Chang profile |
| Electrode dimensions | 114.5 x 14.5 x 2.8 cm |
| Electrode gap | 5 cm |
| Gas chamber volume | $2.6 \times 10^5 cm^3$ |
| Beam area | 5 x 5 cm |
| Discharge volume | 100 x 5 x 5 cm |
| Peak current density | $37\ A/cm^2$ |
| Average electric field at peak current | $\sim$ 11 kV/cm |
| Ionization method | Self-synchronizing side-arcs |
| Input energy density | 300 J/litre |
| Output energy / Discharge volume | 12 J/litre |
| Pulse repetition | 3 shots/minute |

## Appendix B

### Electrical Characteristics

| | |
|---|---|
| Stored energy (at 60 kV) | 792 J |
| Total capacitance | 0.44μF |
| Maximum charging voltage* | 60 kV |
| Typical working voltage* | 55 kV |
| Total peak current at 55 kV* | 18.6 kA |
| Total circuit inductance (in Situ) | 630 nH |
| Current risetime | 280 nsec |
| Current pulse duration | 600 nsec |

*The values of voltage quoted are the static values across the capacitors. On initiation of the discharge, the voltage is doubled across the electrodes.

Appendix C

List of Major Component Specifications
Prices and Suppliers

a. Marx Bank Capacitors :

LCC high voltage film (0.22μF ±10%. 60 kV)

L.C.C. - C.I.C.E., 128 rue de Paris, 93104 Montreuil / France
Swiss Agent : Modulator, Bern
Quantity : 2 off. Price : 1,532.-- SFr. (each)

b. Preionization Capacitors :

Sprague high voltage ceramic. Type 715C 009 571 D8 403 CP.
(570 pF, 40 kV)

Sprague Electric Co., North Adams, Massachusetts 01247 / U.S.A.
Swiss Agent : Telion, Zurich

Quantity 100 off. price : 10.75 SFr. (each)

c. Dump Resistors :

Ceramcarb heavy duty linear resistors. L31 25.10 100 Ohm ± 20%

Power Development Ltd., Cadmore Lane, Cheshunt, Herts., EN8 9SE
England

Quantity 100 off. Price : 6.- SFr. (each)

Appendix D

Gas Mixture and Additive Specifications

The laser is usually run with a 25 : 25 : 50 ($CO_2$, $N_2$,He) Mix. Premixed bottles are used, supplied by Carbagas, Lausanne. Of the three possible grades of purity (Industrial, Pure, Ultra-Pure) it is the Pure grade that is used. The specifications of this grade are as follows :

| | |
|---|---|
| Helium | 99,996 % pure |
| Main impurities : | < 5 ppm $O_2$ |
| | < 5 ppm $H_2O$ |
| | < 1 ppm Hydrocarbons |
| | < 1 ppm $H_2$ |
| Nitrogen | 99,995 % pure |
| Main impurities : | <10 ppm $O_2$ |
| | <10 ppm $H_2O$ |
| Carbon Dioxide | 99,9 % pure |
| Impurities : | < 0,1 % inert gases |
| | <60 ppm $H_2O$ |

Tolerance in the gas mixture ratio ± 10 %.

Bottle capacity : 50 litres filled to 120 bars (with typical flow rates of ∿1 litre/min, this is sufficient for 2-3 weeks operation)

Price : SFr. 120.--

Additive Tri-n-propylamine $(CH_3\ CH_2\ CH_2)_n$ ; purity > 98%

Produced by FLUKA A.G., Buchs SG, Switzerland

Price : SFr. 5.-- for 25 ml (sufficient for more than 1 year)